An ultra-compact planar bandpass filter with open-ground spiral for wireless application

Ma, Kaixue; Yeo, Kiat Seng; Ma, Jianguo; Do, Manh Anh

2008

Ma, K., Yeo, K. S., Ma, J. G., & Do, M. A. (2008). An ultra-compact planar bandpass filter with open-ground spiral for wireless application. IEEE Transactions on Advanced Packaging, 31(2), 285-291.

https://hdl.handle.net/10356/93081

https://doi.org/10.1109/TADVP.2008.920372

An Ultra-Compact Planar Bandpass Filter With Open-Ground Spiral for Wireless Application

Kaixue Ma, *Member, IEEE*, Kiat Seng Yeo, Jian-Guo Ma, *Senior Member, IEEE*, and Manh Anh Do, *Senior Member, IEEE*

***Abstract*—A common via filter is investigated and designed by using a proposed scalable lumped circuit model. The model-based result of the filter agrees well with that of the measurement. An ultra-compact open-ground spiral filter is proposed based on the common via filter. The open-ground spiral resonators are used to design second-order and fourth-order bandpass filters. The filter layouts, which affect filter performance in both passband and stopband, are investigated. The advantages of the open-ground spiral filter include not only its ultra-compact size (only $0.024\lambda_0 \times 0.025\lambda_0$) but also its additional transmission zero points and controllable stopband.**

***Index Terms*—Bandpass filter, odd- and even-mode, open-ground spiral resonator, scalable circuit model, separate electric and magnetic coupling paths, zero point.**

I. Introduction

With the expanding applications of mobile radio communication, a compact size and low cost of passive filters have become very important for miniaturized communication systems. Many publications in the literature have reported on how to reduce the filter size without sacrificing the filter performance [1]–[13]. Normally, a quarter-wavelength resonator [10], [11] has a smaller size as compared to the half-wavelength resonator [1]–[3] or dual-mode ring resonator [4], [5]. Recently, the common via configuration filter with source-load coupling was introduced in [14] to reduce the filter size and improve the performance. A novel method of separate electric and magnetic coupling paths (SEMCP) for designing a miniaturized filter with additional zero points was proposed and investigated in a previous paper [15]. Spiral resonators [13] have emerged as one of the most compact resonators [1]. They are competitive in both the size and the *Q*-factor against hairpin resonators [2], [3], [13], including those which have stepped impedance and are folded into a quarter of their total length. Although the spiral resonator with two open ends [13] is investigated extensively, little work has been reported on the design issue of a spiral resonator with open-ground ends, which occupies much less size as compared to the spiral resonator with two open ends under the same operating frequency. In this paper, the filter with open-ground spiral resonators will be analyzed and designed. Different filter layout configurations, which lead to different filter spectrum responses, are also investigated for the first time. A frequency-variant equivalent lumped circuit model is proposed to investigate and design the common via filters and it is also helpful to understand the operation of the common via open-ground spiral filters.

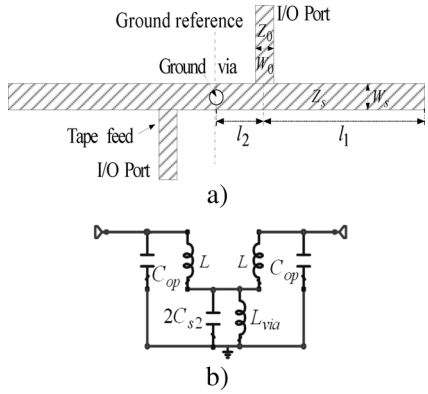

Fig. 1. Second-order filter configuration and its equivalent circuit model. (a) Filter configuration. (b) Equivalent lumped circuit model.

As shown in Fig. 1(a), a microstrip common via bandpass filter is introduced. It consists of two quarter-wavelength resonators and a ground via which is shared by the two resonators along a symmetrical ground reference plane. The ground via provides grounding connections for two quarter-wavelength resonators and generates the required inter-stage coupling for the filter simultaneously. The filter is designed by using a frequency-variant inductance–capacitance (*LC*) equivalent lumped circuit model as shown in Fig. 1(b). The frequency-variant characteristics of resonating elements and interstage coupling of the filter are included in the scalable *LC* circuit model. The good agreement of the measurement and simulation results demonstrates that the proposed frequency-variant *LC* model is applicable for both the analysis and the design. Based on the common via filter, an open-ground spiral resonator is introduced to realize the second-order and fourth-order bandpass filters with ultra-compact size. The layout effect on the filter performance in both the passband and the stopband is investigated. The realized filters demonstrate good selectivity and achieve additional zero points in the stopband.

The paper is arranged as follows: In Section II, the common via bandpass filter and its frequency-variant equivalent circuit model are introduced. The expressions of the element values in equivalent circuit model are derived by using theory of the

Manuscript received May 18, 2006; revised July 24, 2007 and October 9, 2007. This work was recommended for publication by Associate Editor S. Dvorak upon evaluation of the reviewers' comments.

K. Ma is with MEDS Technologies Pte. Ltd, 569876 Singapore (e-mail: kxma@ieee.org).

K. S. Yeo and M. A. Do are with the Center for Integrated Circuits and Systems, Nanyang Technological University, 639798 Singapore.

J.-G. Ma is with the University of Electronic Science and Technology of China, Chengdu 610054, China.

Digital Object Identifier 10.1109/TADVP.2008.920372

transmission line. In Section III, based on the equivalent circuit model, the odd- and even-mode analysis is used to discuss the coupling characteristics, external quality factors, as well as transmission responses. In Section IV, second-order common via filters with open-ground spirals are investigated, designed, and testified by the experiment. In Section V, fourth-order common via open-ground spiral filters are investigated based on full-wave analysis. The fourth-order filters are designed and fabricated to further demonstrate the advantages. The paper is concluded in Section VI.

II. Scalable Model of Filter

According to the transmission line theory, the input admittance of a lossless open-end stub, having characteristic admittance of $Y_s = 1/Z_s$, propagation constant of β_s, and physical length of l_1, as shown in Fig. 1(a), is given by

$$Y_{in} = jY_s \tan(\beta_s(l_1 + \Delta l)) = j\omega C_o \tag{1}$$

where Δl is the equivalent length of the open-end effect as given in the Appendix. The input admittance can be modeled by an admittance of an equivalent capacitance in (1). The equivalent capacitance can be calculated by

$$C_o = \frac{Y_s \tan(\beta_s(l_1 + \Delta l))}{\omega} \quad \text{(F)}. \tag{2}$$

For a section of lossless transmission line with a length of l_2, the transfer matrix is given by

$$\begin{bmatrix} A & B \\ C & D \end{bmatrix}_{s2} = \begin{bmatrix} \cos(\beta_s l_2) & jZ_s \sin(\beta_s l_2) \\ jY_s \sin(\beta_s l_2) & \cos(\beta_s l_2) \end{bmatrix}. \tag{3}$$

The above transmission line section can also be modeled as an equivalent *LC* π-network (one inductor with two shunt capacitors on each side of the inductor). The equivalent inductance L and capacitance C_{s2} can be determined by

$$L = \frac{Z_s \sin(\beta_s l_2)}{\omega} \quad \text{(H)} \tag{4}$$

$$C_{s2} = \frac{1 - \cos(\beta_s l_2)}{\omega Z_s \sin(\beta_s l_2)} \quad \text{(F)}. \tag{5}$$

The single ground via can be modeled as lumped elements [17], [18]. For the range of $h < 0.03\lambda_g$ (h is the thickness of the substrate, and λ_g is the guided wavelength), an accurate and relative simple closed-form equation for the equivalent inductance is given by [17]

$$L_{\text{via}} = \frac{\mu_0}{2\pi}\left[h \cdot \ln\left(\frac{h + \sqrt{r^2 + h^2}}{r}\right) + \frac{3}{2}(r - \sqrt{r^2 + h^2})\right] \quad \text{(H)} \tag{6}$$

where r is the radius of the via. From the above analysis, the structure in Fig. 1(a) can be modeled as a lumped equivalent circuit, as shown in Fig. 1(b). The capacitance C_{op} is calculated by

$$C_{op} = C_o + C_{s2}. \tag{7}$$

Since distributed characteristics of transmission lines and fringe field effects at the open ends are considered in the deduction, the filter in Fig. 1(a) can be modeled by a frequency-variant *LC* network as shown in Fig. 1(b) under lossless conditions with the same accuracy as the transmission line simulators.

III. Model-Based Filter Design

By using even- and odd-mode analysis [6], the odd- and even-mode resonant frequencies of the filter model in Fig. 1(b) can be determined by (8) and (9), respectively

$$\omega_{\text{odd}} = \frac{1}{\sqrt{LC_{op}}} \tag{8}$$

$$\omega_{\text{even}} = \frac{1}{\sqrt{(L + 2\Delta)C_{op}}} \tag{9}$$

where Δ can be calculated by

$$\Delta = \frac{L_{\text{via}}}{1 - \omega^2(2C_{s2}L_{\text{via}})}. \tag{10}$$

The center frequency of the bandpass filter can be approximated by averaging the even- and odd-mode frequencies [9] as

$$\omega_c = \frac{1}{2}(\omega_{\text{even}} + \omega_{\text{odd}}) = \frac{1}{2}\left[\frac{1}{\sqrt{LC_{op}}} + \frac{1}{\sqrt{(L + 2\Delta)C_{op}}}\right]. \tag{11}$$

The coupling between the two resonators is characterized by the coupling coefficient K [8], [9], which can be computed by using the knowledge of the even- and odd-mode frequencies

$$K = \frac{\omega_{\text{odd}}^2 - \omega_{\text{even}}^2}{\omega_{\text{odd}}^2 + \omega_{\text{even}}^2} = \frac{\Delta}{2L + \Delta}. \tag{12}$$

For a narrow-band operation, the external Q-factor (13) of the tapped line quarter-wavelength resonator can be extracted from the circuit model as

$$Q_e = \frac{\omega_c C_{op}}{G_s} \tag{13}$$

where G_s is the admittance of the source. The interstage coupling parameter for second-order quarter-wavelength filter function is given by [8]

$$K = \frac{\pi w}{4\sqrt{g_1 g_2}} \tag{14}$$

where g_1 and g_2 are the element values of the low pass filter prototype, and w denotes the fractional bandwidth. The required value of coupling is computed using (14). This value of coupling is used to find the proper dimensions of the element impedance L_{via} using (6) and (12).

The external Q-factor of the resonator is given by [8]

$$Q_e = \frac{g_0 g_1}{w} = \frac{g_2 g_3}{w}. \tag{15}$$

The Q_e value is used to determine the position of the tape feed using (13).

The above model-based derivation is convenient for the initial design of the filter. To get the frequency response for the whole

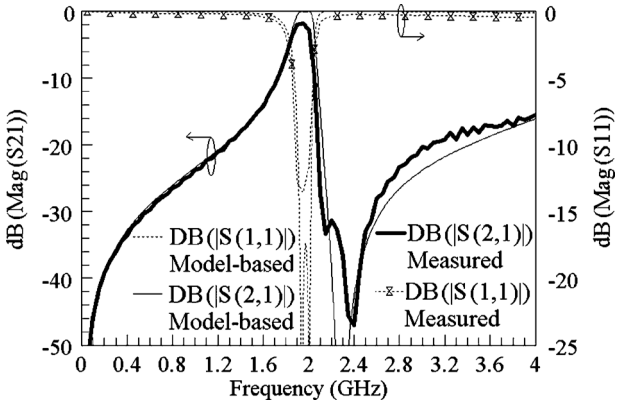

Fig. 2. Comparison of model-based design results and experiment results of filter: $l_2 = 1.55$ mm, $l_1 = 12.25$ mm, $W_0 = Ws = 0.6$ mm, $r = 0.1$ mm.

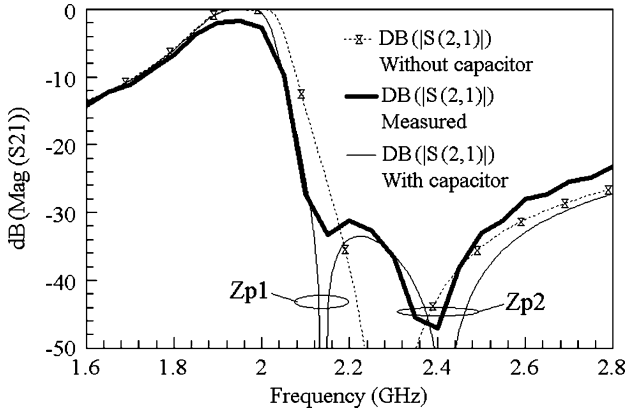

Fig. 3. Comparison of theoretical results with and without electric coupling capacitor and experiment results of the proposed filter.

frequency range, two-port network parameters are used and the transfer matrix of the model in Fig. 1(b) can be calculated by

$$\begin{bmatrix} T_{11} & T_{12} \\ T_{21} & T_{22} \end{bmatrix} = \frac{1}{s\Delta} \begin{bmatrix} 1 & 0 \\ sC_{op} & 1 \end{bmatrix} \times \begin{bmatrix} s(\Delta+L) & s^2L(2\Delta+L) \\ 1 & s(\Delta+L) \end{bmatrix} \begin{bmatrix} 1 & 0 \\ sC_{op} & 1 \end{bmatrix} \quad (16)$$

where

$$T_{11} = T_{22} = \left((L+\Delta) + s^2LC_{op}(L+2\Delta)\right)/\Delta \quad (17)$$

$$T_{12} = \left(sL(L+2\Delta)\right)/\Delta \quad (18)$$

$$T_{21} = \left(2sC_{op}(L+\Delta) + s^3LC_{op}^2(L+2\Delta) + 1/s\right)/\Delta. \quad (19)$$

The transmission and reflection characteristics can be determined by

$$S_{21} = \frac{2}{2T_{11} + T_{12}/Z_0 + T_{21}Z_0} \quad (20)$$

$$S_{11} = \frac{T_{12}/Z_0 - T_{21}Z_0}{2T_{11} + T_{12}/Z_0 + T_{21}Z_0} \quad (21)$$

where Z_0 is the characteristic impedance of the input/output (I/O) feed lines.

The RT/Duroid 6010 laminates from Rogers Corporation with relative permittivity of $\varepsilon_r = 10.2$ and thickness of 0.635 mm is used in our design and analysis. The model-based simulations are performed in Matlab 6.5 from Mathworks, Inc. The effect of the open ends on filters performance shows that there is a slight shift down of the operating frequency. From our investigation, the frequency responses can be accurately characterized even above the second passband. The frequency-variant lumped *LC* model, whose characteristics are different from the traditional frequency-invariant lumped *LC* model, can accurately describe the characteristics of the filter. In Fig. 2, the model-based results are compared with the measured results. Both results are in good agreement in the passband as well as in the stopband. The measured specifications of the filter are: operating frequency 1.94 GHz, 3-dB bandwidth, 160 MHz, and insertion loss 1.75 dB. The stopband attenuation is larger than 30 dB from 2.12 to 2.56 GHz. The rejection at the first zero point of 2.15 GHz and the second zero point of 2.4 GHz are 33 and 47 dB, respectively.

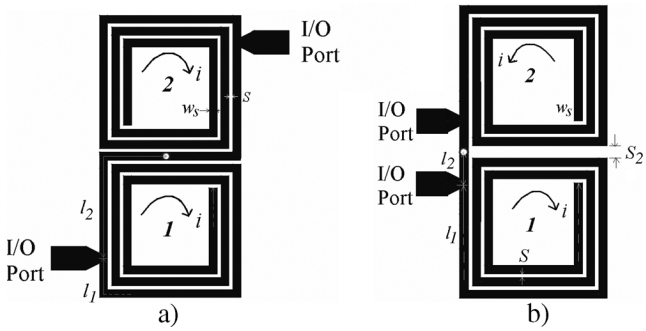

Fig. 4. Configurations of second-order open-ground spiral filter. (a) Inverse layout. (b) Confront layout.

Note: i represents direction of vector current with time count of 0.25.

However, the measured results show two zero points in the high stopband, while the model-based results have only one deep zero point at the high stopband. Meanwhile, the bandwidth of the model-based results is a little larger than that of the measured results in the high passband. The discrepancies are further investigated. It is found that the weak mutual coupling in the space, which is mainly dominant by electric coupling, can shift down the odd-mode frequency and is not considered in the model-based circuit design. So, the operating bandwidth of the measurement is a little reduced as compared to that of the simulation. The dominant magnetic coupling and the weak electric coupling in space cancel out in the high stopband. Thus, the additional zero point in the high stopband is generated [15]. To demonstrate this effect, a small capacitor with a capacitance of 0.013 pF is added between the two open ends. In Fig. 3, the simulated results of the filter with and without the capacitor are compared with the measured result. The small capacitance, which represents the weak electronic coupling of the two resonators through the space, can shift down the odd-mode frequency. It can also reduce the bandwidth and increase the skirt selectivity by generating additional zero point Zp1.

IV. Second-Order Filter Realization

To reduce the size of the filter in Fig. 1(a), the quarter-wavelength resonators are wound as dual-spiral configuration as demonstrated in Fig. 4(a) and (b), respectively. Each spiral, called open-ground spiral, has a short end and an open end. The

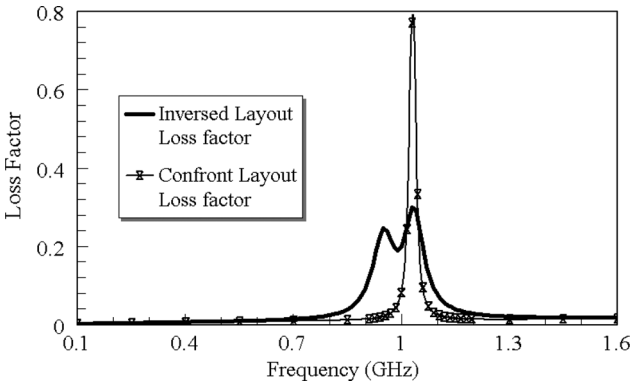

Fig. 5. Comparison of loss factors of open-ground spiral filters in Fig. 4(a) and 4(b). Dimension Fig. 4(a): trace width $Ws = 0.21$ mm, gap between two adjacent trace $S = 0.1$ mm, $l_1 = 28.5$ mm, $r = 0.1$ mm, $l_2 = 3.8$ mm. Dimension Fig. 4(b): trace width $Ws = 0.21$ mm, gap between two adjacent trace $S = 0.1$ mm, $l_1 = 26.7$ mm, $r = 0.1$ mm, $l_2 = 1.2$ mm, distance between two spiral $S_2 = 0.29$ mm.

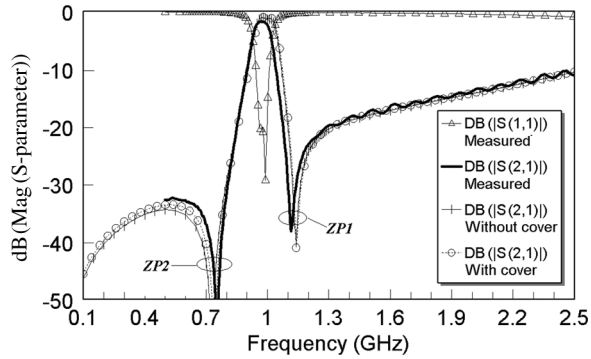

Fig. 6. Comparison of simulated and measured results of second-order open-ground spiral bandpass filter.

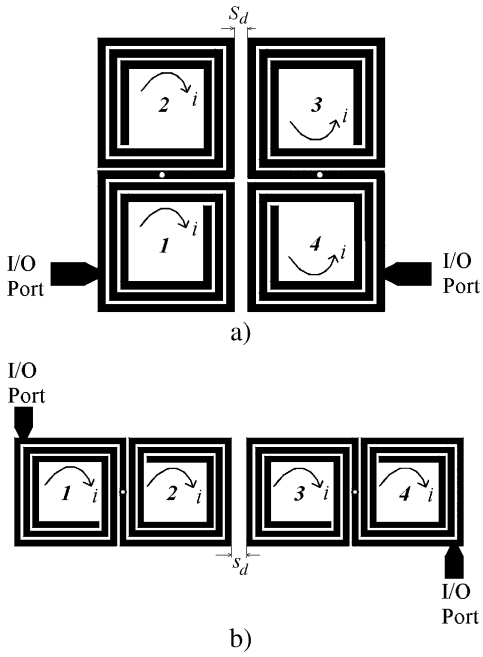

Fig. 7. Two configurations of fourth-order open-ground spiral filters. (a) Hybrid layout. (b) Inverse layout.

Note: i represents direction of vector current with time count of 0.25.

wound metal traces of the open-ground spirals introduce complex distributed effect. Its interaction with adjacent traces and spirals, including mutual capacitance and mutual inductance, are increased. The circuit model in Fig. 1(b) can be applied to get the approximate operating frequency of the spiral resonator and filter. For an accurate design, a full-wave electromagnetic (EM) simulator HFSS [16] is employed to investigate the filters in Fig. 4(a) and (b). Most of the analysis is qualitative, since the fields are three dimensional. They are not easily analyzed, except those by computer simulation, which are well documented in [8] and [9]. The loss factors $(1 - |S_{11}|^2 - |S_{21}|^2)$ of the two filters in Fig. 4(a) and (b) are compared in Fig. 5. At the operating frequencies, both filters have return loss better than 13 dB. It is interesting to note that the loss factors at the operating frequencies are dramatically different. From the current distribution at the operating frequencies, it can be found that the difference comes from the mutual magnetic coupling between two spiral resonators. For the inverse layout illustrated in Fig. 4(a), the mutual magnetic coupling between resonators 1 and 2 is enhanced according to the current distribution and the Faraday's law. Thus, the radiation loss is reduced. However, for the confront layout, the mutual magnetic flux between resonators 1 and 2 in Fig. 4(b) is cancelled by the self magnetic flux of the resonator. This will increase the radiation and the eddy-current loss. The confront layout is not good for the filter design and it will not be elaborated upon further. The inverse layout in Fig. 4(a) is an obvious advantage for the filter design. The results of the second-order filter in Fig. 4(a) with 10% fractional bandwidth are compared in Fig. 6. The simulated and measured results are in close agreement. The simulated results with and without metal cover (the height of the shielding box is 6 mm) demonstrate that shielding has less of an effect on the performance of the filter. The filter characteristics are shown in Fig. 6. The generation of additional zero points can be interpreted by the canceling effect in separate electric and magnetic coupling paths as discussed in [15]. The qualitative analysis of the zero points generation is quite complex. The measured minimum insertion loss of the filter is only 1.8 dB and the return loss in passband is better than 15 dB. The rejection of the two zero points in low and high stopbands are 53 and 37 dB, respectively. The occupied active area (without considering the I/O feed lines) is only $0.024\lambda_0 \times 0.012\lambda_0$ (λ_0 is the free space wavelength at the operating frequency).

V. Fourth-Order Filter Realization

The open-ground spiral resonators are also used to build up two fourth-order bandpass filters, as illustrated in Fig. 7(a) and (b). The initial coupling parameters for filter design can be synthesized from the general coupling matrix and the interstage coupling coefficient between the open-ground spiral resonators can be determined by the resonant frequencies using the full wave EM extraction procedure [9]. The passband characteristics are mainly decided by the coupling parameters of the coupling matrix, while the stopband characteristics are determined not only by the coupling parameters but also by the layout of the resonators and filter. That is because the interstage

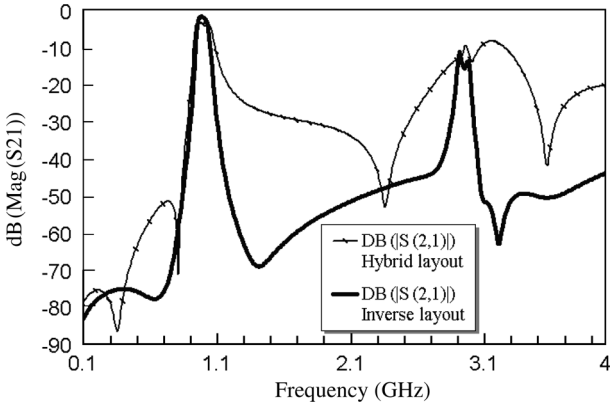

Fig. 8. Simulated results of two fourth-order open-ground spiral filters. Dimensions of open-ground spiral: trace width $Ws = 0.21$ mm, gap between two adjacent trace $S = 0.1$ mm, $r = 0.1$ mm—for Fig. 7(a): $l_2 = 4.2$ mm; $l_1 = 28.1$ mm, $S_d = 0.35$ mm and for Fig. 7(b): $l_2 = 5.0$ mm, $l_1 = 27.3$ mm, $S_d = 0.5$ mm.

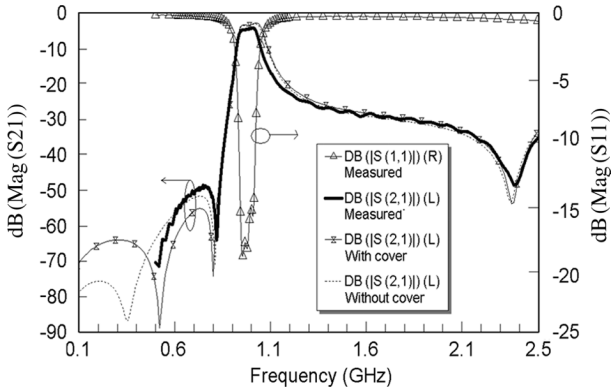

Fig. 9. Comparison of simulated and measured results of fourth-order open-ground spiral filter.

coupling between any two open-ground spiral resonators is frequency dependent. Moreover, both the cross-coupled resonators and resonators with the separate electric and magnetic coupling paths [15] can generate additional zero points in the stopband. The coupling characteristics of the adjacent open-ground spiral resonators are difficult to analyze qualitatively. The full wave EM results of two layout conditions are compared in Fig. 8. Both bandpass filters have the center operating frequency of 0.98 GHz. The filter in Fig. 7(b) has lower insertion loss (1.8 dB) in the passband and deeper rejection in high stopband than the filter in Fig. 7(a) (insertion loss of 3.2 dB). The good stopband characteristics of the filter in Fig. 7(b) are due to the canceling effect of the separate electric and magnetic coupling paths [15], which introduces additional zero points in the low stopband and the high stopband. The low insertion loss in the passband is because of the inverse layout, where mutual magnetic coupling between any two adjacent open-ground spiral resonators (denoted as resonators 1, 2, 3, 4) is enhanced and relative low radiation loss is achieved. The hybrid filter layout in Fig. 8(a) has an inverse layout between resonators 1 and 2 as well as between resonators 3 and 4. But the confront layout between resonators 1 and 4 as well as between resonators 2 and 3, as discussed in Section IV, has more loss compared to inverse layout.

The EM results with and without cover (the height of the shielding cover is still 6 mm) are compared with the measured results of the filter in Fig. 7(a). Fig. 9 shows that the simulated results are in good agreement with the measured results, and the cover effect on the filter performance is mainly at the zero point in the low stopband below 0.6 GHz. Two additional zero points are generated and the rejection and rolloff in low stopband are quite good. The measured results of the fourth-order filter are shown in Fig. 9. The measured insertion loss is around 4.2 dB, the return loss is better than 15 dB, and the rejection in low stopband is better than 49 dB. The size of the fabricated fourth-order bandpass filter occupies an active area as small as $0.024\lambda_0 \times 0.025\lambda_0$ (0.72×0.76 cm $= 0.55$ cm^2). The filter in Fig. 7(b) is not fabricated. However, by comparing the simulated results in Fig. 8 and the measured results in Fig. 9, the insertion loss of the filter in Fig. 7(b) is expected to be around 2.8 dB.

VI. Conclusion

In this paper, a scalable model for the common via filter is introduced. The open-ground spiral filters are proposed based on the common via filter. The zero point generation mechanism of the second-order filters and fourth-order filters is investigated. The radiation characteristics of the filters with different layouts are compared and discussed. The second-order and fourth-order planar bandpass filters operating around 900 MHz with ultra-compact size are implemented on low-cost printed circuit boards (PCBs). The open-ground spiral filter can also be built using superconducting technology to further improve the filter performance [13].

Appendix

At the open end of a microstrip line with width W and substrate thickness h, the field does not stop abruptly but extends slightly further due to the effect of the fringing field [18]. This effect can be modeled as an equivalent transmission line with length Δl

$$\Delta l = hP_1P_3P_5/P_4 \tag{22}$$

where

$$P_1 = 0.434907\frac{\varepsilon_{re}^{0.81} + 0.26(W/h)^{0.8544} + 0.236}{\varepsilon_{re}^{0.81} - 0.189(W/h)^{0.8544} + 0.87}$$

$$P_2 = 1 + \frac{(W/h)^{0.371}}{2.35\varepsilon_r + 1}$$

$$P_3 = 1 + \frac{0.5274\tan^{-1}\left[0.084(W/h)^{1.9413\cdot P2}\right]}{\varepsilon_{re}^{0.9236}}$$

$$P_4 = 1 + 0.037\tan^{-1}\left[0.067(W/h)^{1.456}\right] \cdot \{6 - 5\exp\left[0.036(1-\varepsilon_r)\right]\}$$

$$P_5 = 1 - 0.218\exp(-7.5\,W/h).$$

For the range of $0.01 \le W/h \le 100$ and $\varepsilon_r \le 128$, the accuracy is better than 0.2%.

Acknowledgment

The authors would like to thank K. T. Chan of MEDs Technologies Pte., Ltd., Singapore for his help in the fabrication.

REFERENCES

[1] S. B. Cohn, "Parallel-coupled transmission-line resonator filters," *IRE Trans. Microwave Theory Tech.*, vol. 6, no. 4, pp. 223–231, Apr. 1958.

[2] E. G. Cristal and S. Frankel, "Hairpin-line and hybrid hairpin-line half-wave parallel-coupled-line filters," *IEEE Trans. Microwave Theory Tech.*, vol. 20, no. 11, pp. 719–728, Nov. 1972.

[3] M. Sagawa, K. Takahashi, and M. Makimoto, "Miniaturized hairpin resonator filters and their application to receiver front-end MIC's," *IEEE Trans. Microwave Theory Tech.*, vol. 37, no. 12, pp. 1991–1996, Dec. 1989.

[4] I. Wolff, "Microstrip bandpass filter using degenerate modes of microstrip ring resonator," *Electron. Lett.*, vol. 8, no. 12, pp. 779–781, Jun. 1972.

[5] L. Zhu and K. Wu, "A joint field/circuit design model of microstrip ring dual-mode filters: Theory and experiments," in *Proc. Asia-Pacific Microwave Conf.*, 1997, pp. 865–868.

[6] I. C. Hunter, *Theory and Design of Microwave Filters*. Stevenage, U.K.: IEE, 2001.

[7] C.-H. Wang, Y.-S. Lin, and C. H. Chen, "Novel inductance-incorporated microstrip coupled-line bandpass filters with two attenuation poles," in *IEEE MTT-S Int. Symp. Dig.*, 2004, pp. 1979–1982.

[8] J.-S. Hong and M. J. Lancaster, *Microstrip Filters for RF/Microwave Applications*. New York: Wiley, 2001.

[9] G. L. Matthaei, L. Young, and E. M. T. Jones, *Microwave Filters, Impedance-Matching Networks, and Coupling Structures*. Dedham, MA: Artech, 1964.

[10] J. Zhou, M. J. Lancaster, and F. Huang, "Coplanar quarter-wavelength Quasi-elliptic filters without bond-wire bridges," *IEEE Trans. Microwave Theory Tech.*, vol. 52, no. 4, pp. 1150–1156, Apr. 2002.

[11] T. Kitamura, Y. Horii, M. Geshiro, and S. Sawa, "A dual-plane comb-line filter having plural attenuation poles," *IEEE Trans. Microwave Theory Tech.*, vol. 50, no. 4, pp. 1216–1219, April 2004.

[12] G. L. Matthaei, "Narrow-band, fixed-tuned, and tunable bandpass filter with zig-zag hairpin-comb resonators," *IEEE Trans. Microwave Theory Tech.*, vol. 51, no. 4, pp. 1214–1219, Apr. 2003.

[13] F. Huang, "Ultra-compact superconducting narrow-band filters using single-and twin-spiral resonators," *IEEE Trans. Microwave Theory Tech.*, vol. 51, no. 2, pp. 487–491, Feb. 2003.

[14] K. Ma, J.-G. Ma, M. A. Do, and K. S. Yeo, "A novel compact two-order bandpass filter with three zero points," *IEE Electron. Lett.*, vol. 41, no. 15, pp. 846–848, Jul. 2005.

[15] K. Ma, J.-G. Ma, K. S. Yeo, and M. A. Do, "A compact size coupling controllable filter with separated electric and magnetic coupling paths," *IEEE Trans. Microwave Theory Tech.*, vol. 54, no. 3, pp. 1113–1119, Mar. 2006.

[16] Ansoft HFSS, Version 9.2 Ansoft Corporation. Pittsburgh, PA.

[17] M. E. Goldfarb and R. A. Pucel, "Modeling via hole grounds in microstrip," *IEEE Microwave Guided Wave Lett.*, vol. 1, no. 6, pp. 135–137, Jun. 1991.

[18] D. G. Swanson, "Grounding microstrip lines with voles," *IEEE Trans. Microwave Theory Tech.*, vol. 40, no. 8, pp. 1719–1721, Aug. 1992.

[19] M. Kirschning, R. H. Jansen, and N. H. L. Koster, "Accurate model for open end effect of microstrip lines," *Electron. Lett.*, vol. 17, no. 3, pp. 123–125, Feb. 1981.

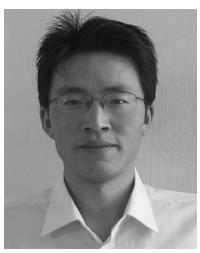

Kaixue Ma (S'05–M'05) received the B.Sc. and M.Eng. degrees from Northwestern Polytechnical University (NWPU), Xi'an, China, in 1997 and 2002, respectively, and the Ph.D. degree from Nanyang Technological University (NTU), Singapore, in 2007, all in electrical engineering.

From 1997 to 2002, he was with 504th of China Academy of Space Technology (CAST), where he was Deputy Director of millimeter-wave group involved in products development and R&D projects of microwave and millimeter-wave components and subsystem for satellite payload. From 2004 to 2005, he investigated 60-GHz front-end system and mixer designs in the Wireless Communication Laboratory, NICT. From 2005 to 2007, he was with MEDs Technologies as an R&D Manager, where he did projects and design services and developed products for WiMAX equipment used by Agilent Malaysia and parallel test modules of 10-Gb/s optical transceivers supplied to AVAGO Singapore. Since September 2007 to the present, he has been with ST Electronics, Singapore, as an Research and Development Manager and Project Leader to develop a $2 \sim 30$ GHz ultra-wide bandwidth software defined radio system. His research interests include software defined radio, high frequency circuits and system design, and packaging using advanced technologies. He filed two patents and has published more than 20 papers in related areas.

Dr. Ma is a member MTT-S and ComSOC. He is a Reviewer of several international journals. He received the Best Technical Paper Award by CAST in 2002.

Kiat Seng Yeo received the B.Eng. (with honors) degree and the Ph.D. degree in electrical engineering, both from Nanyang Technological University (NTU), Singapore, in 1993 and 1996, respectively.

He began his academic career at NTU as a Lecturer, in 1996, and was promoted to Assistant Professor, in 1999, and then to Associate Professor, in 2002. He was Sub-Dean of Student Affairs from 2001 to 2005. During this period, he held several concurrent appointments as Program Manager of the system-on-chip flagship project, Coordinator of the integrated circuit design research group, and Principal Investigator of the integrated circuit technology research group at NTU. He is on the advisory committee of the Centre for Science Research and Talent Development of Hwa Chong Junior College and Consultant/Advisor to statutory boards and multinational corporations in the areas of semiconductor devices, electronics, and integrated circuit design. He has authored three books: *Low-Voltage, Low-Power VLSI Subsystems* (McGraw-Hill, 2005), *Low-Voltage Low-Power Digital BiCMOS Circuits: Circuit Design, Comparative Study, and Sensitivity Analysis* (Prentice Hall, 2000), and *CMOS/BiCMOS ULSI: Low-Voltage, Low-Power* (Prentice Hall, 2002). The latter was translated into a Chinese version. He has filed/granted more than six patents and published over 200 articles on CMOS/BiCMOS technology and integrated circuit design in leading technical journals and conferences worldwide.

Dr. Yeo was the Technical Chair of the 8th and 9th International Symposium on Integrated Circuits, Devices and Systems (ISIC-1999 and ISIC-2001) and he also served on the program committee of the International Symposium on VLSI Technology, Systems, and Applications (VLSI-TSA), Taiwan, R.O.C., and the International Symposium on Low-Power and High-Speed Chips (COOL Chips), Japan, 1999 and 2002, respectively. He has been appointed Head of Circuits and Systems for a period of three years from July 2005. He is a Technical Reviewer for several prestigious international journals.

Jian-Guo Ma (M'96–SM'97) received the B.Sc. and M.Sc. degrees (with honors) from Lanzhou University, Lanzhou, China, in 1982 and 1988, respectively, and the Doctoral degree in engineering from Gerhard-Mercator University, Duisburg, Germany, in 1996.

From January 1982 to March 1991, he was with Lanzhou University, where he was involved with RF and microwave engineering. Prior to joining Nanyang Technological University, Singapore, in 1997, he was with the Technical University of Nova Scotia, Halifax, Canada. He was an Associate Professor and Director of the Center for Integrated Circuits and Systems, Nanyang Technological University of Singapore. Since 2005, he has been with the University of Electronic Science and Technology of China (UESTC), Chendu, China. He has authored or coauthored over 180 technical papers and two books. He holds six patents in CMOS RF integrated circuits (RFICs). His research interests include RF integrated-circuit RFIC designs for wireless applications, RF characterization and modeling of semiconductor devices, RF interconnects and packaging, system-on-chip applications, electromagnetic compatibility/electromagnetic interference in RFICs, and monolithic-microwave integrated-circuit applications.

Manh Anh Do (SM'90) received the B.Sc. degree in physics from the University of Saigon, in 1969, and BE and Ph.D. degrees, both from University of Canterbury, New Zealand, in 1973 and 1977, respectively.

Between 1977 and 1989, he held various positions including: Design Engineer, Production Manager, and Research Scientist in New Zealand, and Senior Lecturer at National University of Singapore. He joined the School of Electrical and Electronic Engineering, Nanyang Technological University (NTU), Singapore, as a Senior Lecturer, in 1989, and obtained the Associate Professorship, in 1996, and Professorship, in 2001. Currently, he is the Director of Centre for Integrated Circuits and Systems, NTU. He has been a Consultant for many projects in the electronic industry and was a key consultant for the implementation of the $200 million Electronic Road Pricing (ERP) project in Singapore, from 1990 to 2001. His current research is on mobile communications, RFIC design, mixed-signal circuits and intelligent transport systems. Before that, he specialized in sonar designing and biomedical signal processing. He has authored and coauthored over 200 papers in the areas of electronic circuits and systems. Between 1995 and 2005, he was Head of Division of Circuits and Systems, NTU.

Dr. Do was a council member of IET, U.K., from 2001 to 2004, and an Associate Editor for the IEEE TRANSACTIONS ON MICROWAVE THEORY AND TECHNIQUES, in 2005 and 2006. He is a Fellow of IET and a Chartered Engineer.